Influence of the molecular weight on mechanical behavior and associated strain-induced structural evolution of Poly(ethylene 2,5-furandicarboxylate) upon biaxial stretching

G. Stoclet, S. Xu, V. Gaucher, J.F. Tahon, S. van Berkel, A. Arias, C. Rogeret, R. Nourichard, S. de Vos

Influence of the molecular weight on mechanical behavior and associated strain-induced structural evolution of Poly(ethylene 2,5-furandicarboxylate) upon biaxial stretching

G. Stoclet[1*], S. Xu[1], V. Gaucher[1], J.F. Tahon[1], S. van Berkel[2], A. Arias[2], C. Rogeret[1], R. Nourichard[1], S. de Vos[2].

[1] Univ. Lille, CNRS, INRAE, Centrale Lille, UMR 8207 - UMET - Unité Matériaux et Transformations, F-59000 Lille, France

[2] Corbion Purac BV, Arkelsedijk 46, 4206 AC Gorinchem, The Netherlands.

*Corresponding author: gregory.stoclet@univ-lille.fr

Abstract:

The mechanical behavior of Poly(ethylene 2,5-furandicarboxylate) upon biaxial stretching and the associated strain-induced structural evolution is studied in the light of its molecular weight. Besides it is shown that the increase of molecular weight favors strain-induced crystallization (SIC) and that SIC in PEF occurs when a critical molecular orientation ratio is achieved. The earlier occurrence of SIC in the case of the higher macromolecular weight is explained by the faster macromolecular orientation due to a more robust entanglement network.
Regarding the mechanical behavior, it appears that a strain-hardening stage is observed whatever the molecular weight, this stage originates from both macromolecular orientation and formation of crystals upon stretching. Finally, it is shown that biaxial orientation (BO) has a positive effect on both oxygen barrier properties and mechanical properties. Particularly it was highlighted that, while as-cast PEF is brittle, BO PEF films are ductile when a critical biaxial draw ratio is achieved.

Keywords: biaxial stretching, Poly(ethylene 2,5-furandicarboxylate), macromolecular orientation, crystallization, barrier properties.

Introduction:

Poly(ethylene 2,5-furandicarboxylate) (PEF) knows an increasing interest due to, on the one hand its bio-based nature and, on the other hand, its interesting properties that could allow it to be used in a large field of applications such as packaging[1]. Due to their similar chemical nature, PEF is often compared to poly(ethylene terephthalate) (PET). Several studies have been carried out regarding the characterization of the PEF physical properties. These works have shown that PEF exhibits similar thermal properties as PET, i.e., a glass transition temperature (T_g) around 80°C, a melting temperature (T_m) in the 220-250°C temperature range and slow thermal crystallization kinetics[2,3,4,5,6,7]. The same can be said about the mechanical properties[8], which are somewhat equivalent between the two polymers. However, as a main feature, PEF exhibits significantly better

water and gas barrier properties in comparison with PET, which is explained by the reduced chain mobility of PEF as compared to PET.[9,10,11]

Several studies have been published regarding the mechanical behavior of PEF upon uniaxial stretching in the rubbery state[12,13,14,15,16,1718]. They underlined the fact that the microstructure induced upon stretching is strongly dependent on the stretching conditions and that the strain-hardening of the material, observed for some stretching conditions, is linked to the formation of an ordered structure (crystalline or mesomorphic) upon stretching[11,12]. These studies also showed that the content of ordered structure induced by uniaxial stretching could reach 35% [16] and that the crystalline structure involved is different from the one induced by thermal crystallization[12]. Regarding the relationships between mechanical behavior and structural evolution, Mao et al. have shown that local ordering of the chains occurs before the occurrence of strain-induced crystallization (SIC). They also pointed out that the onset of strain-hardening occurs in the meantime that strain-induced crystallization[13] suggesting a link between these two phenomena. On the other hand, in a recent study, Forestier et al. clearly demonstrate that PEF crystals are formed before the occurrence of structural hardening and that the PEF strain-induced crystallization process exhibits a "simple" two-steps path with no intermediate phases stable with no formation of intermediate order phase[16].

Beyond uniaxial stretching, biaxial stretching is also of prime interest as it allows to simulate industrial processes such as bottle stretch-blow molding, biaxial film drawing or thermoforming. Regarding biaxial stretching of PEF, only an explorative study from van Berkel et al. has, to date, addressed this topic. In their work, van Berkel and his coworkers compared the mechanical behavior and the structural evolution in the rubbery state of PEF with that of PET[19]. They observed that strain-hardening and strain-induced crystallization appear at higher stretching ratios for PEF than for PET. This retarded occurrence of strain-hardening in the case of PEF is ascribed to its higher mass between entanglements, as compared to PET. Besides they assume that in order to achieve the same amount of entanglement per chain, and consequently a comparable network of entanglements, a higher molecular weight for PEF is needed to meet the behavior of PET. In addition they also observe that, in like for uniaxial stretching[12], the content of the crystalline phase induced upon stretching in the case of PEF is low (around 10% maximum). Finally, they observed that biaxial orientation has a beneficial impact on both mechanical and gas barrier properties of PEF, although the impact on barrier properties is significantly lower than in the case of PET. In particular they noted an increase of tensile modulus and tensile strength for the biaxially oriented films as well as some decrease of both O_2 and CO_2 permeability, even if limited.

Basically, this work of van Berkel et al. is the first one giving information about i) the mechanical behavior of PEF upon biaxial stretching and ii) the influence of biaxial orientation on the structure of PEF. However, in their study, only PEF samples with high biaxial orientation degrees, comparable to the ones encountered in industrial conditions, have been characterized. Consequently the whole process of strain-induced structural evolution during biaxial stretching remains unaddressed. In particular the origin of the strain-hardening upon biaxial stretching in the case of PEF remains unclear. Several studies dealing with the link between strain-hardening and SIC have been carried out in the case of other polymers[20,21,22,23,21,22,23,24,25]. For example, Chandran et al. carefully analyzed the influence of the stretching conditions on both strain-hardening and strain-induced crystallization[24] of PET and directly linked both phenomena. Similar studies carried out with PLA, an aliphatic crystallizable bio-based polyester, lead to the same conclusions[25,26]. In other words these studies indicate that strain-hardening originates from SIC. Nevertheless, on the other hand, studies carried out on atactic polystyrene (i.e. which is not able to crystallize) demonstrate that strain-hardening results from the extension of the entanglement network[27,28]. Consequently, even if PEF seems to

have a behavior close to the one of PET, determining the origin of PEF's strain-hardening, and the respective contribution of amorphous orientation and SIC on the mechanical behavior, could be of prime interest.
Another unaddressed point regarding the PEF mechanical behavior and associated structural evolution is the effect of molecular weight. As suggested in [16], the later occurrence of strain-hardening in the case of PEF as compared to PET is due to its higher M_e. As suggested by van Berkel et al., this should be balanced by the achievement of a comparable network of entanglements (i.e. the achievement of the same amount of entanglements per chain) by increasing the molecular weight as already shown in the case of PET[29].

As a consequence, this study is devoted to determine the structure – mechanical behavior relationships of PEF upon biaxial stretching above T_g in order to determine the origin of the strain-hardening. In addition, the influence of molecular weight on mechanical behavior of PEF and on the associated strain-induced structural evolution will be studied in order to determine if this parameter allows to tune the mechanical behavior of PEF towards the one of PET.

Experimental:

- ✓ Materials and elaboration

Three different neat Poly(ethylene 2,5-furandicarboxylate) polymer samples with different molecular weights, supplied by Corbion, have been used. The polyesters were made by classical esterification-polycondensation in the presence of a Sb_2O_3 catalyst and SSP was applied when needed to increase Mw. Their respective molecular weight values are listed in Table 1.

Abbreviation	M_n (kg/mol)	M_w (kg/mol)	M_w/M_n	Average number of entanglements per chain
LMW-PEF	23	39	1.7	≈ 6.5
MMW-PEF	32	54	1.74	≈ 9
HMW-PEF	51	89	1.76	≈ 14.5

Table 1 : Molecular characteristics of the PEF resins used.

The average number of entanglements per chain has been calculated as Mn/Me with Me the average molecular weight between entanglements, taken equal to 3500 g/mol from [15].

For sake of clarity the PEF exhibiting the lowest molecular weight will be denoted LMW-PEF, the one having the intermediate molecular weight will be denoted MMW-PEF and finally the material having the highest molecular weight will be denoted HMW-PEF.

Resins were dried before extrusion below a moisture content of 50 ppm, as determined Karl Fischer. Extruded cast films of the three resins have been elaborated using as single screw extruder. The melt temperature was maintained at 255 °C for the LMW and MMW samples, for the HMW sample a melt temperature of 280 °C was applied. The obtained cast was cooled using a 30 °C cooling drum. The average obtained sample width was 14 cm, and the thickness was around 400 microns.

Biaxial stretching

A Brückner Karo IV laboratory biaxial stretcher was used for the biaxial drawing of the specimens. Experiments were carried out on 10x10 cm² squares cut from the extruded films (thickness from 300

to 500µm). Simultaneous biaxial stretching was carried out at drawing temperatures (T_d) of 100 °C using an initial stretching speed ($\dot{\varepsilon} = \frac{deformation\ rate}{initial\ length}$) of 200%.s^{-1}. Viscoelastic properties measurements have been carried out in order to ensure that, for these stretching conditions, the material is in its rubbery state (see Fig SI.1)

Finally elongation ratios λ_{MD} x λ_{TD} up to 4.5x4.5 were tested.
The mechanical behavior is represented by:

- The elongation ratio : $\lambda_{xx} = \frac{l}{l^0}$ with l^0 the initial length of the sample
- The true stress calculated as: $\sigma_{xx} = \frac{F_{xx}}{S}$ with F_{xx} the applied force in the *xx* direction and S the cross-section calculated assuming the hypothesis of constant volume deformation.

Prior to biaxial stretching the samples were heated during 30 s at T_d in order to reach thermal equilibrium. The three principal axes of the films are defined as the machine direction (MD) which correspond to the extrusion direction, the transverse direction (TD) which corresponds to the direction perpendicular to the extrusion direction in the film plane and the normal direction (ND) which is the direction perpendicular to the film place. Regarding the mechanical behavior during biaxial stretching, for sake of clarity, only the stress recorded along the machine direction (MD) will be reported in the mechanical behavior plots. However, it was ensured for each test that the same behavior was recorded along the machine and the transversal direction (MD and TD). Finally, in order to ensure that stretching is homogeneous, an ink grid composed of 1x1cm² squares has been printed onto the film and analyzed after the film stretching.

Thermal properties and Crystallization kinetics analyses

Thermal properties of the materials were determined by means of Differential Scanning Calorimetry (DSC) analyses. A DSC Q20 (TA Instruments) apparatus was used. Temperature and heat flow were calibrated with a high purity indium sample using standard procedures. Experiments were carried out under nitrogen flow on about 10mg samples placed in aluminum crucibles. Isothermal crystallization kinetics from the melt at 165°C of the PEF films were determined using the following thermal cycle:

- Holding the sample at 280°C during 2min.
- Cooling down to 165°C at 50K/min.
- Isothermal during 120min.
- Cooling down to 25°C at 50K/min.
- Isothermal during 1min at 25°C
- Heating up to 280°C at 10K/min

Viscoelastic properties measurement

Dynamic Mechanical Analyses were carried out on a RSA III apparatus from TA Instruments operated in tensile mode. Experiments were performed at the frequency of 1Hz, between 25°C to 180°C at a heating rate of 5°C.min^{-1}. Rectangular shaped samples with length and width of 20 x 6 mm² respectively were cut from PEF films.

Macromolecular orientation: Trichroic Infrared Analyses

The Fourier Transform Infrared (FTIR) spectra were collected in transmission mode on a Bruker VERTEX 70v spectrometer equipped with a DTGS detector and a rotating polarizer. Every FTIR spectrum consisting of 64 scans was recorded over the wavenumber range 550–3500 cm^{-1} with a resolution of 2 cm^{-1}. In our study trichroic infrared measurements were adopted to assess the orientation functions for biaxially stretched samples with a 3D texturing nature. For spectra along stretch axis, S_M and S_T were measured with the polarization parallel to the M and T directions respectively where reduced absorbance were recorded.

In order to obtain the spectrum S_N through the film thickness, trichroic analysis was carried out by tilting the films about the T axis at 45° with respect to the IR beam, and the spectrum S_{MN} was measured with the polarization in the MN plane. Then, the S_N spectrum corresponding to a polarization through the thickness was computed from the following relation

$$S_N = (2n^2)\sqrt{1-\frac{1}{2n^2}} \times S_{MN} - (2n^2-1) \times S_M$$

Where *n* is the effective refractive index of the polymer in the direction of the beam propagation. Due to the lack of data regarding the refractive index of PEF, the value of PET (i.e. *n* = 1.58) has been used[30].

Then, the S_0 spectrum for biaxially drawn samples was calculated from the equation

$$S_0 = \frac{1}{3}(S_M + S_T + S_N)$$

Based on the calculated S_0 spectra, a quantification of the macromolecular orientation degree has been performed. The orientation of a molecular chain axis *i* is usually described by three Herman's orientation functions f_{ij} where j = M, T or N holds for the directions defined above. The three orientation functions must obey the relationship

$$f_{iM} + f_{iN} + f_{iT} = 0$$

For a transition moment of an infrared vibration along the molecular axis *i*, the Herman's orientation function can be calculated by means of the following equation

$$f_{ij} = \frac{1}{2}(\frac{A_j}{A_0} - 1)$$

Where A_j and A_0 are the band intensities in the S_j and S_0 spectra respectively and j = M, T or N

For sake of accuracy, the vibration bands used in the calculations should be distinct bands with absorbance below the saturation. In addition, these bands should be sensitive to orientational change, i.e., showing trichroic behavior when 3D texturing is present. In our study, the eligible band showing trichroic behavior is the band at 619 cm^{-1}, assigned to amorphous phase in PEF as once reported in [25].

Structural characterization

WAXS and SAXS measurements were performed on a Xeuss 2.0 apparatus (Xenocs) equipped with a micro source using a Cu K_α radiation (λ= 1.54 Å) and point collimation (beam size: 300×300µm²). The

sample to detector distance, around 12 cm for WAXS and 2.5m for SAXS, is calibrated using silver behenate as standard. Through view 2D diffraction patterns are recorded on a Pilatus 200k detector (Dectris). Integrated intensity profiles are computed from the 2D patterns using the Foxtrot® software.

SAXS experiments were carried out to determine the nature of the plastic deformation mechanism(s) involved during cold drawing. To achieve this goal a homemade stretching device adaptable on the apparatus was used in order to analyze the sample during stretching. Besides, these tensile tests were carried out at room temperature (i.e. 20°C) using an initial stretching speed $\dot{\varepsilon} = 10^{-3}\ s^{-1}$. For the determination of the nature of the plastic deformation mechanism(s) involved, stretching is stopped just before sample's break and the acquisition is done on constrained sample.

Oxygen Transmission Rate measurement

Oxygen transmission rate (OTR) has been analyzed according to the ASTM D3985-17 norm and F1927-14. The film sample was analyzed in duplicate with the Mocon Oxtran 2/22L equipment. When the amount of sample area allowed it, the maximum sample area of 50cm² was used for the OTR measurement. A smaller film area of 5.64cm² was used for other foil samples. The OTR analysis was directly measured with 100% oxygen concentration as permeant gas. Analyses were performed at 23°C and 80% relative humidity. Enough conditioning time was applied to allow the sample to adjust to the relative humidity condition. Test was automatically stopped when the difference between the last 4 cycles of the measurement series showed less than 1% relative difference.

Mechanical properties of biaxially drawn samples

Mechanical properties of biaxially drawn samples were determined via tensile tests upon uniaxial stretching. The tests were performed on an Instron 4466 apparatus at room temperature (i.e. 20°C) using an initial stretching speed $\dot{\varepsilon} = 10^{-3}\ s^{-1}$. For each set of material, at least three dumbbell specimens having 22 mm and 6 mm in gauge length and width respectively were tested.

Results:

Initial materials characterization

Thermal behavior of the three PEF samples has been investigated by means of DSC. Analysis showed that all the cast films are amorphous with a glass transition temperature (T_g) around 84°C ±1°C revealing no significant effect of molecular weight. To complete the potential influence of molecular weight was also investigated regarding its effect on crystallization kinetics and viscoelastic properties. Figure 1 depicts the isothermal DSC thermograms recorded at 165°C after cooling of the samples from the molten state.

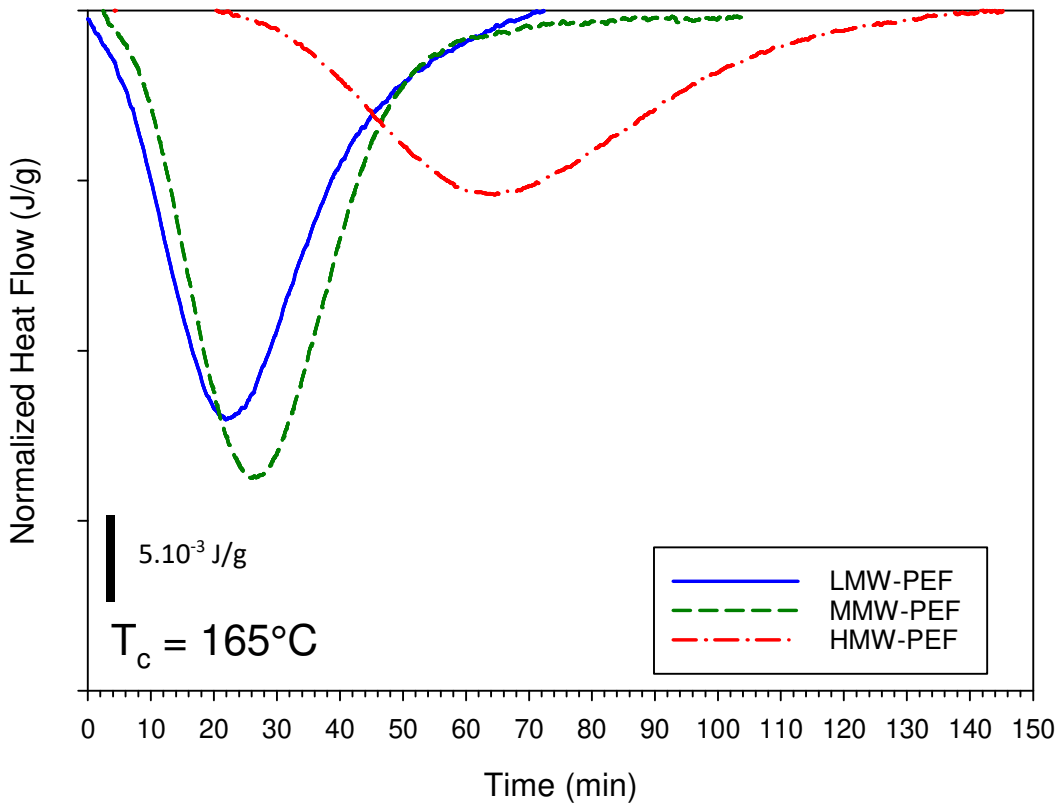

Figure 1: Thermograms recorded during isothermal crystallization from the molten state at T_c = 165°C of LMW-, MMW- and HMW-PEF (endo up).

As can be seen, the crystallization kinetics are roughly similar for both LMW-PEF and MMW-PEF samples, while the one of HMW-PEF is significantly slower. While the crystallization half-time is around 20 and 30 minutes for LMW- and MMW-PEF, respectively, it is around 65 minutes for HMW-PEF. This retarded crystallization for HMW-PEF can be attributed to its higher molecular weight, which involves a decrease of the molecular mobility and thus slower macromolecular rearrangements required for crystal formation under these steady conditions. Even if the molecular weight influences the crystallization kinetics, no differences were observed regarding the crystallinity degree achieved, around 34% ±2% (standard melting enthalpy taken equal to 140 J/g [31]), as well as the melting temperature, around 205°C (DSC thermograms are depicted in Fig SI.2).

Finally the viscoelastic properties of the different materials have also been compared. The evolution of the storage modulus E' for the three different materials is shown in Figure 2.

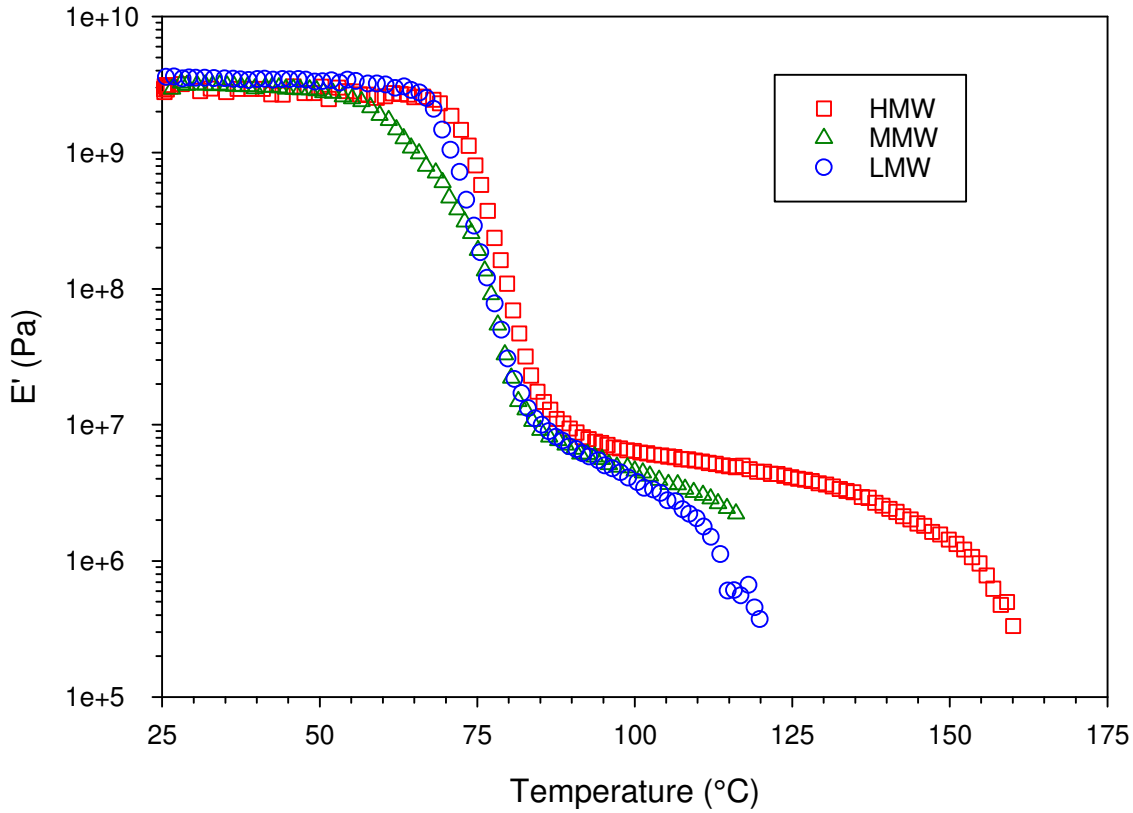

Figure 2: Evolution of the storage modulus E' as a function of the temperature for LMW-, MMW- and HMW-PEFs (heating rate 5°C/min, f = 1Hz)

In the glassy state, the molecular weight has no significant influence on E' as all the materials exhibit a storage modulus around 3GPa. A sharp decrease of E', characteristic of the α relaxation, is also observed around 75°C for the three materials. On the other hand, an influence of the molecular weight can be observed in the rubbery state where a short rubbery plateau is observed for both LMW- and MMW-PEF while it spans a larger temperature range for HMW-PEF. Finally, the terminal transition characterized by the flowing of the sample involving a sharp drop of E' at the end of the rubbery plateau happens at much higher temperature for HMW-PEF due to its much higher molecular weight. On the other hand, LMW- and MMW-PEF have a higher ability towards disentanglement. Indeed for these two materials, the molecular weight is only 3 times higher than the critical mass (Mc = 2Me, with Me ≈ 3500 g/mol[2,32]) to form entanglements while it is 7 times higher for HMW-PEF.

In summary, the characterization of the initial sample materials revealed that LMW- and MMW-PEF exhibit similar thermal and viscoelastic properties, while HMW-PEF differs strongly, as a direct result of its significantly higher molecular weight. Particularly this higher molecular weight leads to a higher number of entanglements per chain and consequently a slower disentanglement rate which explains the larger rubbery plateau.

Mechanical behavior of PEF upon biaxial stretching and associated strain-induced structural evolution

The mechanical behavior upon simultaneous biaxial stretching of LMW-, MMW- and HMW-PEFs has been studied on a wide range of stretching conditions. For sake of clarity, the purpose of the paper being to determine the relationships between the structure and the mechanical behavior of PEF, only the mechanical behavior for some sets of conditions will be presented and discussed here. Figure 3 depicts the mechanical behavior of PEF biaxially stretched according to the stretching conditions for which i) a biaxial stretching ratio of 4.5x4.5 could be achieved whatever the molecular weight and ii) the strain-hardening slope is the higher.

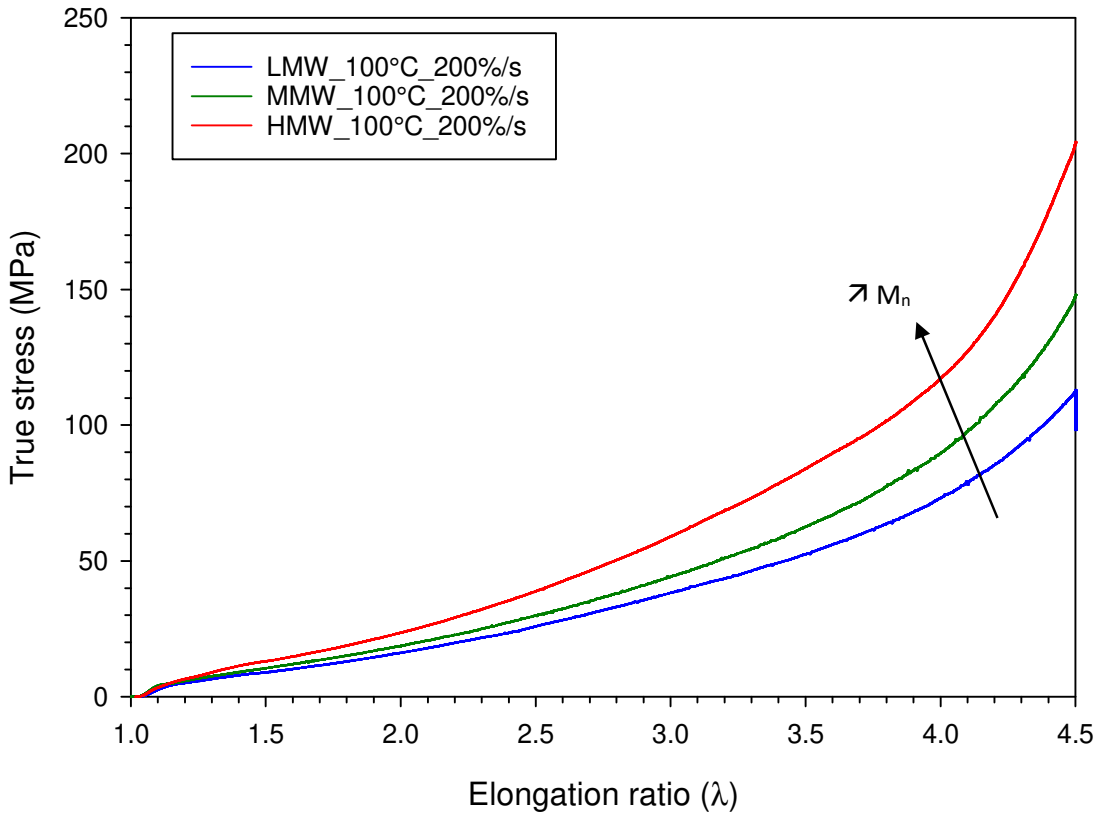

Figure 3: Influence of the molecular weight of PEF on the mechanical behavior during simultaneous biaxial stretching (Td = 100°C, $\dot{\epsilon} = 2s^{-1}$, for sake of clarity only the stress recorded along MD is depicted, however it was ensure that $\sigma_{MD} = \sigma_{TD}$)

The mechanical behavior observed is typical of an initially amorphous polymer stretched in the rubbery state such as PET and similar to the one reported by van Berkel et al in the case of PEF[16]. For all PEF samples, whatever their molecular weight, an elastic region at low strains is observed followed by a deformation zone where stress slowly increases finally followed by a strain-hardening stage where stress rapidly increases with strain. Contrary to the results reported for compression

molded PEF plaques in [16], even if stretching conditions are comparable, a marked strain-hardening is observed in the case of each PEF for $\lambda \geq 4$, comparable to the one reported in PET.

Regarding the effect of the molecular weight, it appears that the increase of the molecular weight involves an increase of the applied stresses. This could be ascribed to the increase of the number of entanglement per chain with the increase of molecular weight which leads to a more robust entanglement network. However, the effect of molecular weight on the onset of strain-hardening appears limited even if a slightly earlier occurrence of strain hardening is observed with the increase of the molecular weight. Nevertheless, even if the effect on the onset of strain-hardening is limited, the increase of molecular weight involves an increase of the strain-hardening slope. Indeed the slope in that region, taken for $4.2 \leq \lambda \leq 4.5$, increases from 0.9 MPa/% to 1.39 MPa/% for MMW-PEF and to 2.14 MPa/% for HMW-PEF. This more pronounced strain-hardening with the increase of the molecular weight has already been reported in the case of PET[33] and PEN[34], but comparisons are difficult as units are not the same or as viscosity values are given rather than molecular weight data. The origin of the effect of molecular weight on the strain-hardening slope will be discussed later in the manuscript.

In order to determine the structural origin of strain-hardening in PEF, and also in order to determine the origin of the molecular weight effect, a particular attention has been paid to the characterization of the biaxially stretched samples.

Indeed, as previously mentioned, strain hardening can have two origins:

- strain-induced crystallization as demonstrated in the cases of PET or PLA
- high extension and solicitation of the entanglement network as for PS, i.e. macromolecular orientation

Structural characterization

The strain-induced structural characterization has been assessed by means of WAXS. Figure 4 depicts the integrated intensity profiles calculated from 2D (face-on) WAXS patterns for the three PEF resins biaxially stretched at different elongation ratios.

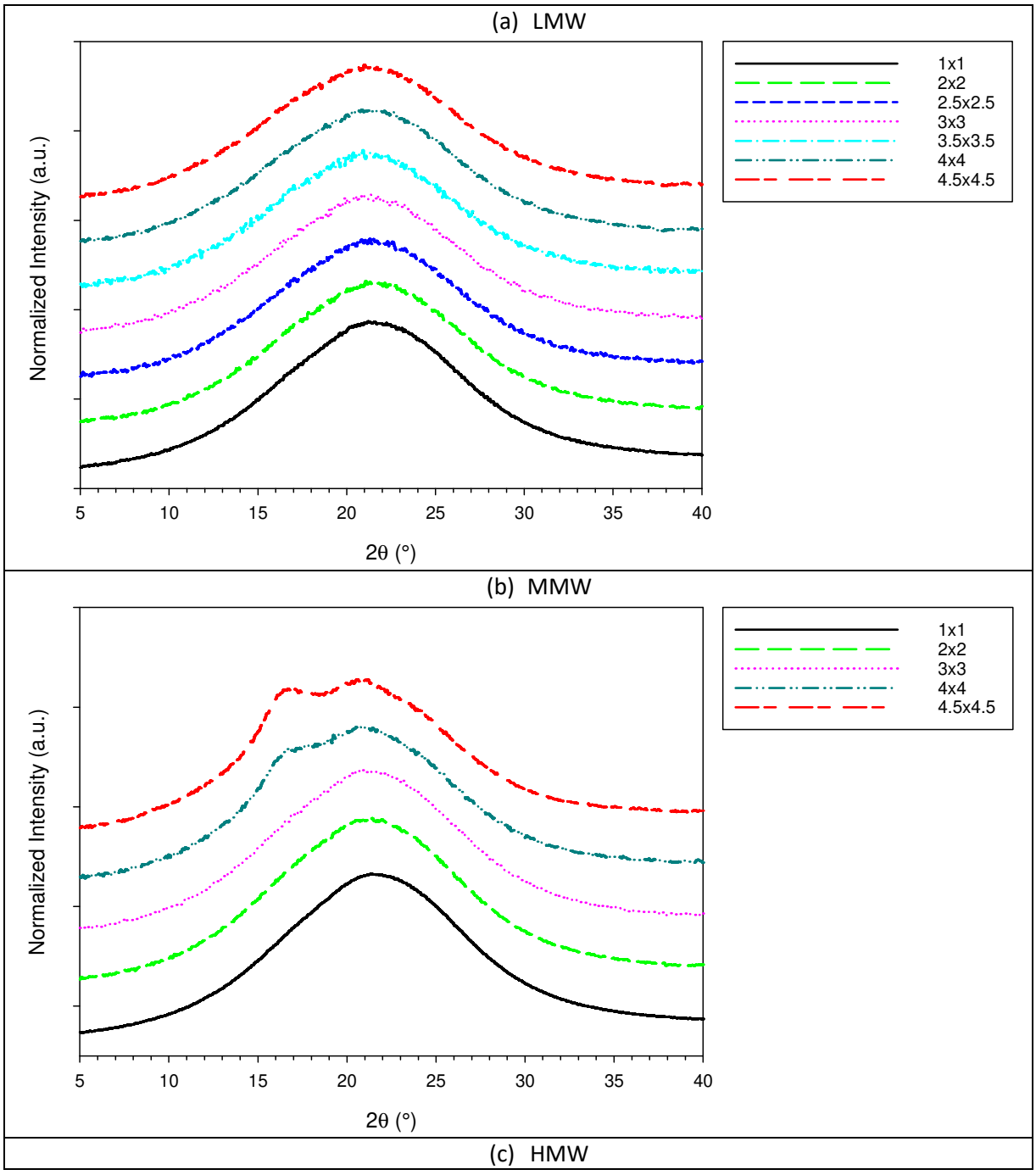
(a) LMW
Normalized Intensity (a.u.)
2θ (°)
5
10
15
20
25
30
35
40
1x1
2x2
2.5x2.5
3x3
3.5x3.5
4x4
4.5x4.5
(b) MMW
Normalized Intensity (a.u.)
2θ (°)
1x1
2x2
3x3
4x4
4.5x4.5
(c) HMW

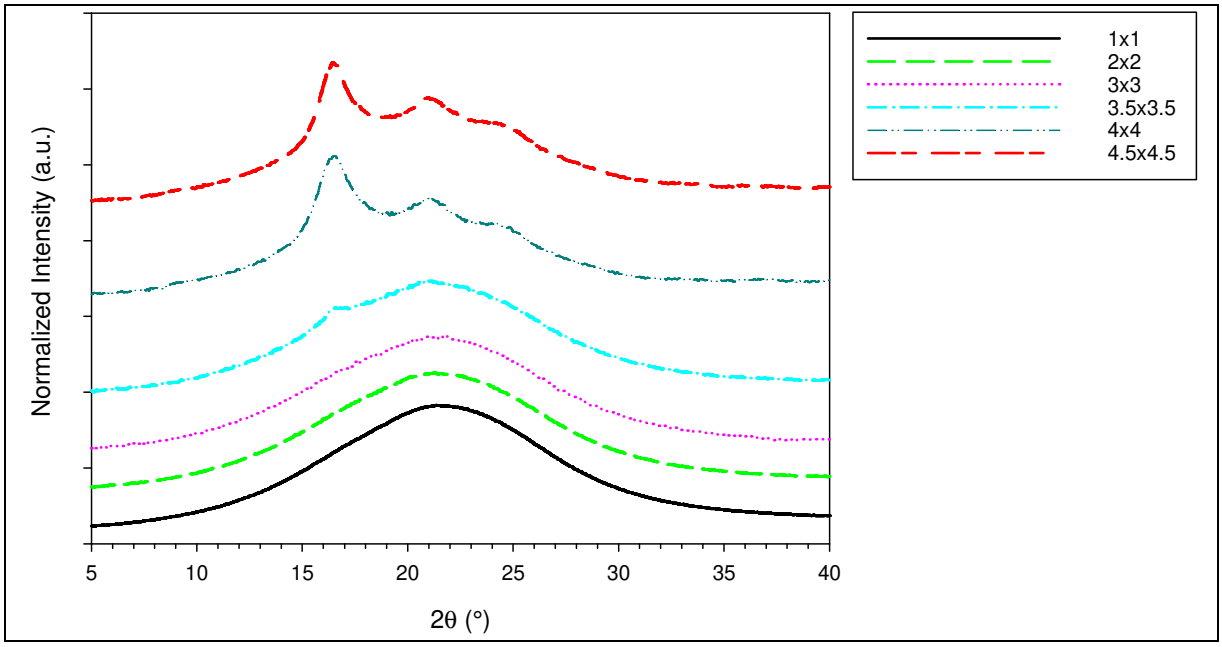

Figure 4: WAXS Integrated intensity profiles as a function of the elongation ratio for (a) LMW-PEF, (b) MMW-PEF and (c) HMW-PEF

It first appears that all the films are initially amorphous whatever the molecular weight which indicates the quenching speed of the cast film during production was sufficient to prevent crystallization. Regarding LMW-PEF, it appears that for these biaxial stretching conditions, the film remains fully amorphous whatever the elongation ratio, even in the strain-hardening region. In the case of MMW-PEF, the appearance of diffraction peaks at 2θ = 16.5° and 2θ = 20.9° is noted for stretch ratios $\lambda x\lambda \geq 4x4$, attesting of the occurrence of a strain-induced crystallization. The intensity of these peaks slightly increases between stretch ratios of 4x4 and 4.5x4.5 even if it remains low, indicating only modest levels of crystallinity. Finally for HMW-PEF, the appearance of diffraction peaks is noted for a stretch ratio of $\lambda x\lambda$ = 3.5x3.5. The intensity of these peaks drastically increased in the stretched film with areal stretch ratio 4x4 and then remains roughly constant at 4.5x4.5. Consequently, results indicate that the increase of molecular weight allows for, and even favors, the strain-induced crystallization process of these cast PEF films.

It can be noted that for MMW- and HMW-PEF the onset of strain-induced crystallization roughly corresponds to the onset of the strain-hardening. However, even if a strain-hardening stage is observed for LMW-PEF, no strain-induced crystals were detected. To go further, the crystalline structure induced by biaxial stretching has been analyzed by means of 2D-WAXS and 2D-SAXS. Regarding SAXS (data not shown here) no scattering characteristic of the presence of stacked crystals was observed whatever the sample.

As an illustration, Figure 5 depicts the 2D face- and edge-on WAXS patterns obtained on HMW-PEF biaxially stretched up to $\lambda x\lambda$ = 4.5x4.5.

HMW-face (beam along ND)	HMW-edge (beam along MD)

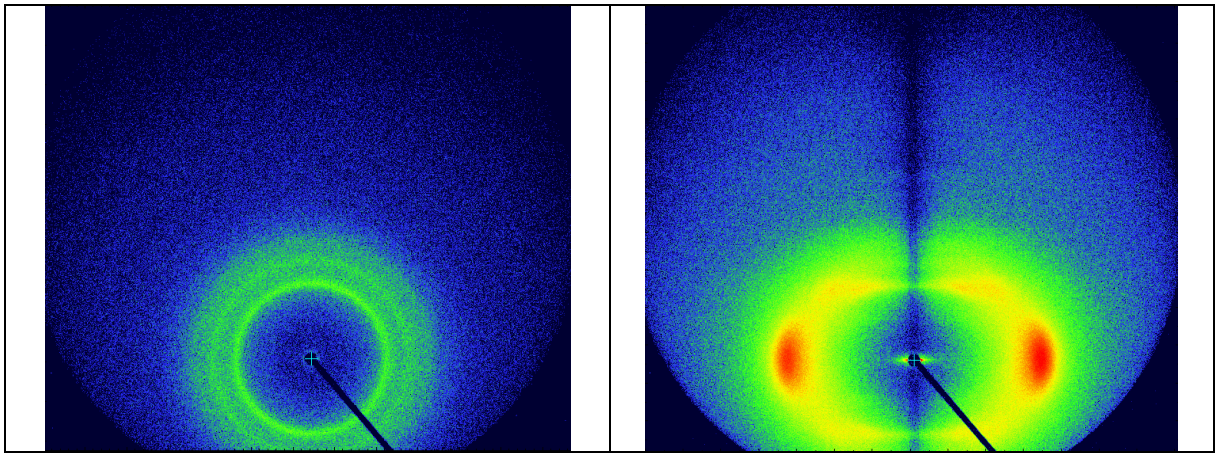

Figure 5: (a) face-on and (b) edge-on WAXS patterns of HMW-PEF biaxially stretched up to λxλ = 4.5x4.5.

Regarding the WAXS pattern recorded along ND, isotropic diffraction rings are observed. On the other hand diffraction arcs are observed on the pattern recorded along MD. This clearly shows that the crystalline structure induced upon biaxial stretching is orthotropic, i.e., PEF crystals lie parallel to the film plane. This particular crystalline orientation, often encountered in the case of biaxially oriented polymer, should probably play a role in the improvement of barrier properties previously reported[16], by restricting segmental motion of amorphous chain parts arrested by microcrystals.

The type of crystalline structure involved by biaxial stretching has been also assessed. Figure 6 depicts the comparison between thermally crystallized PEF and PEF having crystallized upon biaxial stretching.

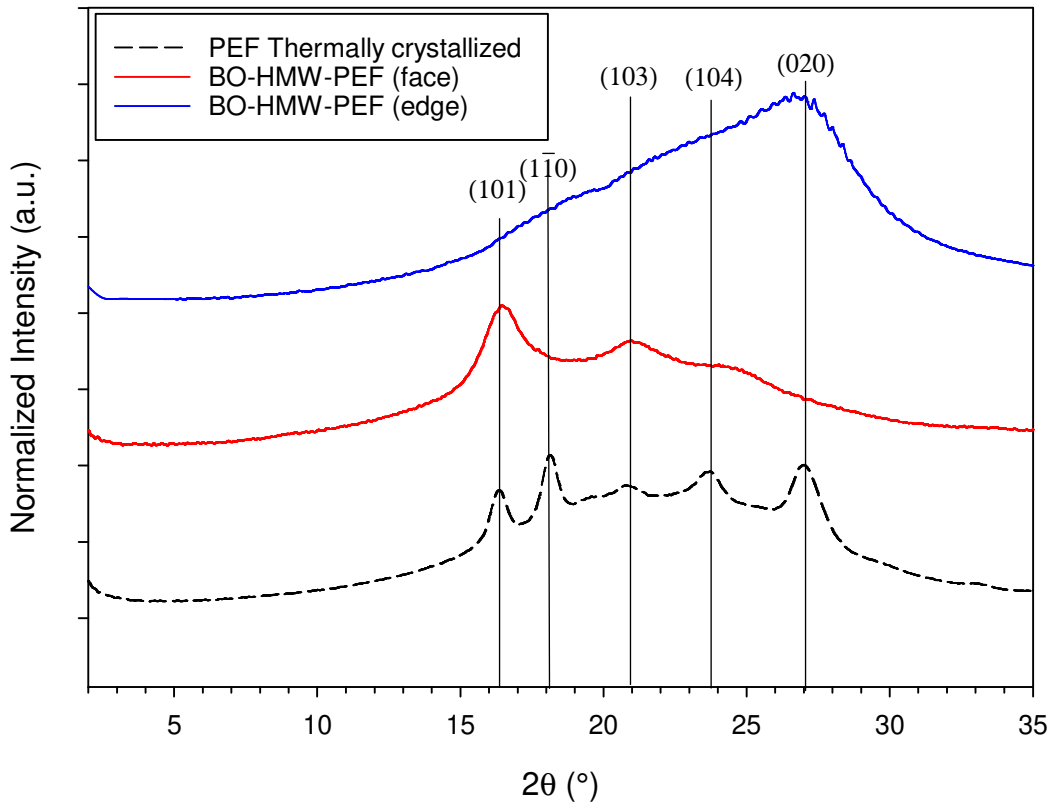

Figure 6: integrated intensity profiles of thermally crystallized PEF and biaxially oriented HMW-PEF (sample biaxially stretched up to λxλ = 4.5x4.5 at 100°C and $\dot{\varepsilon} = 200\%/s$, the indexation of the diffraction peaks has been made on the basis of the results from [17]).

The comparison seems to show a satisfactory agreement between the position of the diffraction peaks of the thermally crystallized and "biaxially crystallized samples" indicating that it is the "standard" α or α' crystalline form which is induced upon biaxial stretching. For uniaxial stretching, on the contrary it has been reported that the crystalline structure differs from the α or α' structure[12]. Indeed the two characteristic peaks observed at 2θ = 3.2° and 2 θ = 6.4° in uniaxially stretched PEF are not seen in this biaxially oriented sample. This shows that the nature of the molecular orientation process, i.e., uniaxial or biaxial, indeed plays a key role on the nature of the crystalline phase induced.

In order to complete this study, the evolution of the amorphous microstructure upon biaxial stretching has also been assessed using FTIR measurements. In order to determine the contribution of the macromolecular orientation of the amorphous chains to the mechanical behavior, the Herman's orientation parameter of the amorphous macromolecules has been determined for the three biaxially stretched materials up to different elongation ratios. Figure 7 depicts the Wilchinksi diagrams of the orientation functions of the PEF with different molecular weights and the evolution of the orientation parameter as a function of the elongation ratio.

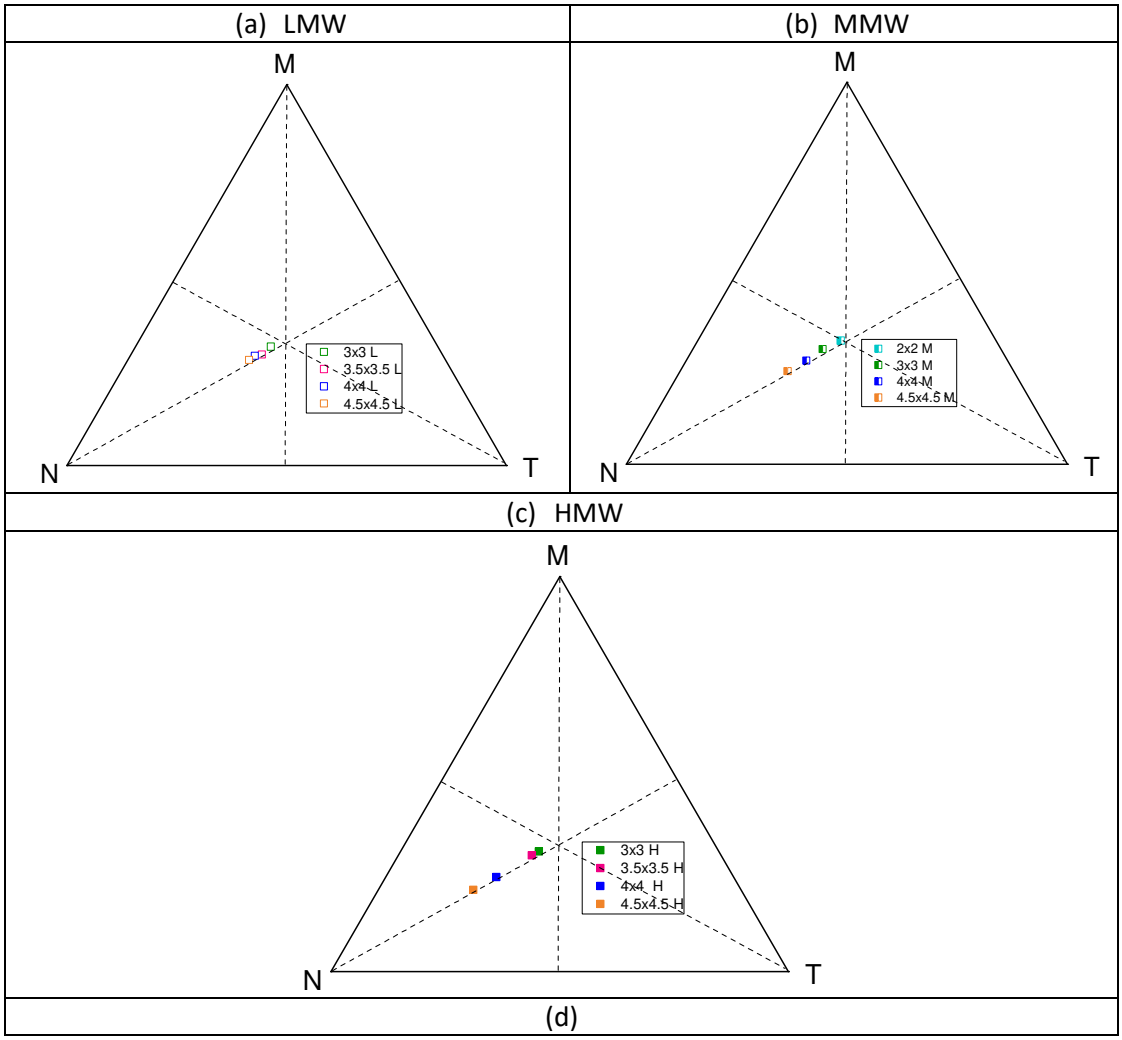

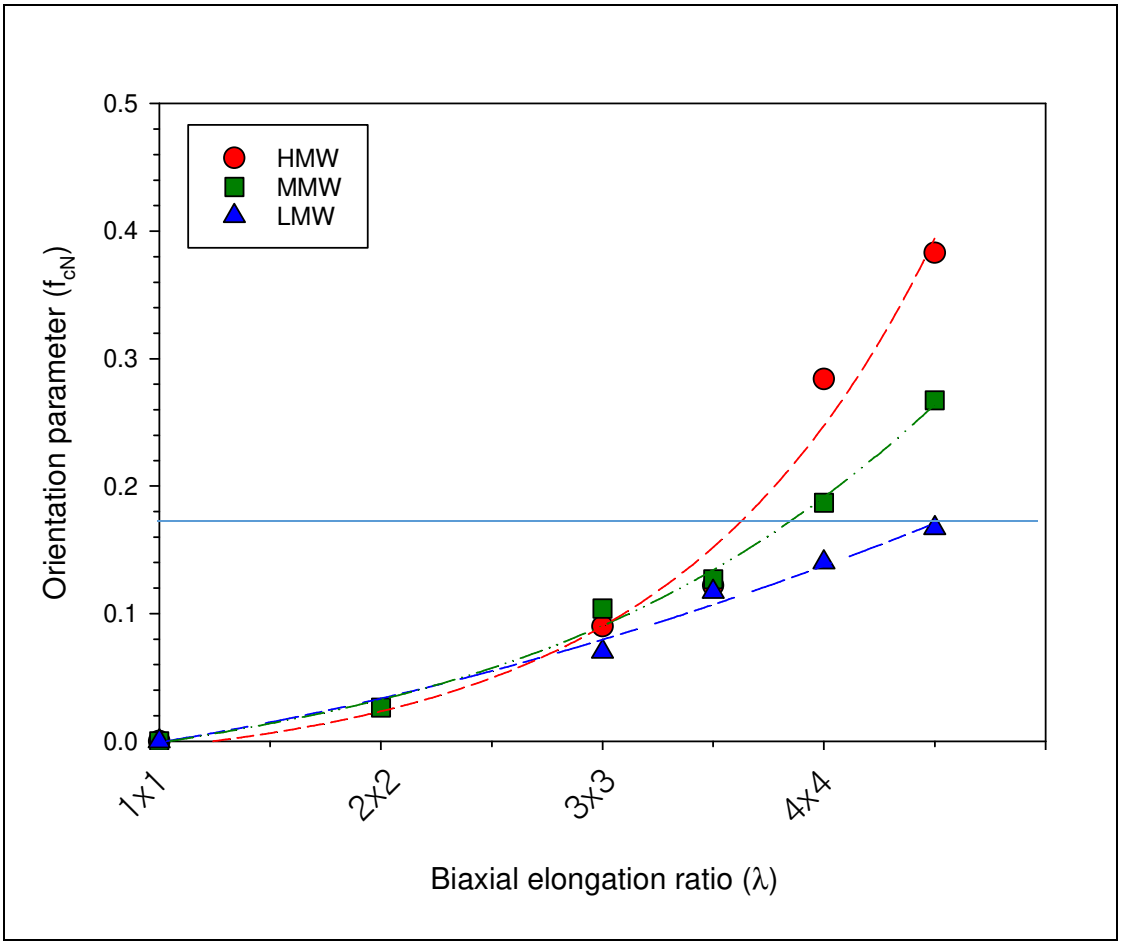

Figure 7: Wilchinski diagrams of the orientation function for biaxially stretched (a) LMW-PEF, (b) MMW-PEF, (c) HMW-PEF and (d) evolution of the orientation parameter f_{cN} as a function of the elongation ratio (The line represents the critical value of the orientation parameter above which SIC is observed).

Figure 7 (a)-(c) reveal that the evolution of the orientation parameter is similar irrespective of molecular weight. The vibration band characteristic for the amorphous phase of PEF at 619 cm^{-1} tends to orient towards the normal direction (ND) to the film plane with the increase of the elongation ratio. Since the vibration band considered at 619 cm^{-1} is perpendicular to the chain axis[35], the evolution tendency towards ND indicates in fact that the macromolecules tend to orient in the MT plane during biaxial stretching. In addition the fact that all points fall upon the median of MT plane suggests an equiaxial orientation parameter along MD and TD, however combing the former 2D-WAXS results the overall texture should be "isotropic" in the plane of film.

A quantitative analysis of the evolution of the orientation parameter as a function of strain (Figure 7.d) indicates that the molecular weight has no significant effect until an elongation ratio of 3x3. Up to this areal stretch ratio the orientation parameter monotonously increases with strain. This can be ascribed to the fact that, in this deformation range, the macromolecular network is slightly constrained and plastic deformation rather occurs by chains unfolding and reorganization. Consequently, at this point the fact that LMW-PEF, which exhibits less entanglements per chain, than HMW-PEF does not infer on the mechanical behavior observed. Above this 3x3 elongation ratio indeed significant differences are observed between the PEF samples of different Mw. Especially the orientation parameter strongly increases with strain for HMW-PEF, while it increases slowly with strain for LMW-PEF. This trend is in line with the mechanical behavior of the materials where an increase of the strain-hardening slope was observed with the increase of the molecular weight. This slower orientation for LMW-PEF than for HMW-PEF can be ascribed to the fact that, due to the lower

number of entanglements per chain, the macromolecules have the possibility to slip and to disentangle, which disadvantages macromolecular orientation. In other words, the increase of the molecular weights involves a decrease of the disentanglement rate upon stretching which favors the macromolecular orientation. A comparison with WAXS data also showed that the onset of strain-induced crystallization is observed at the same orientation parameter for both MMW- and HMW-PEF ($f_{cN} \approx 0.18$). This result is of prime interest as it tends to prove the existence of a critical amorphous orientation for the beginning of crystallization, as for PET[36]. This conclusion seems to be confirmed by the behavior of LMW-PEF for which no crystallization was observed and which also exhibit an orientation parameter $f_{cN} \leq 0.18$ over the entire studied areal stretch ratio range.

Finally, a remaining question is the origin of the strain-hardening stage. At this point one can state that both amorphous orientation and presence of crystals are at the origin of the phenomenon. However, later results also show that the presence of crystals involves – and perhaps even facilitates - an increase of the amorphous orientation parameter. Therefore, one can wonder if the slope of the strain-hardening is determined, by the high rigidity of crystals or rather by the fact that the amorphous chains are highly oriented and arrested in a constantly increasing network of crystals. In an attempt to answer this question, the evolution of the slope in the strain-hardening region has been plotted as a function of f_{cN}, as depicted in Figure 8.

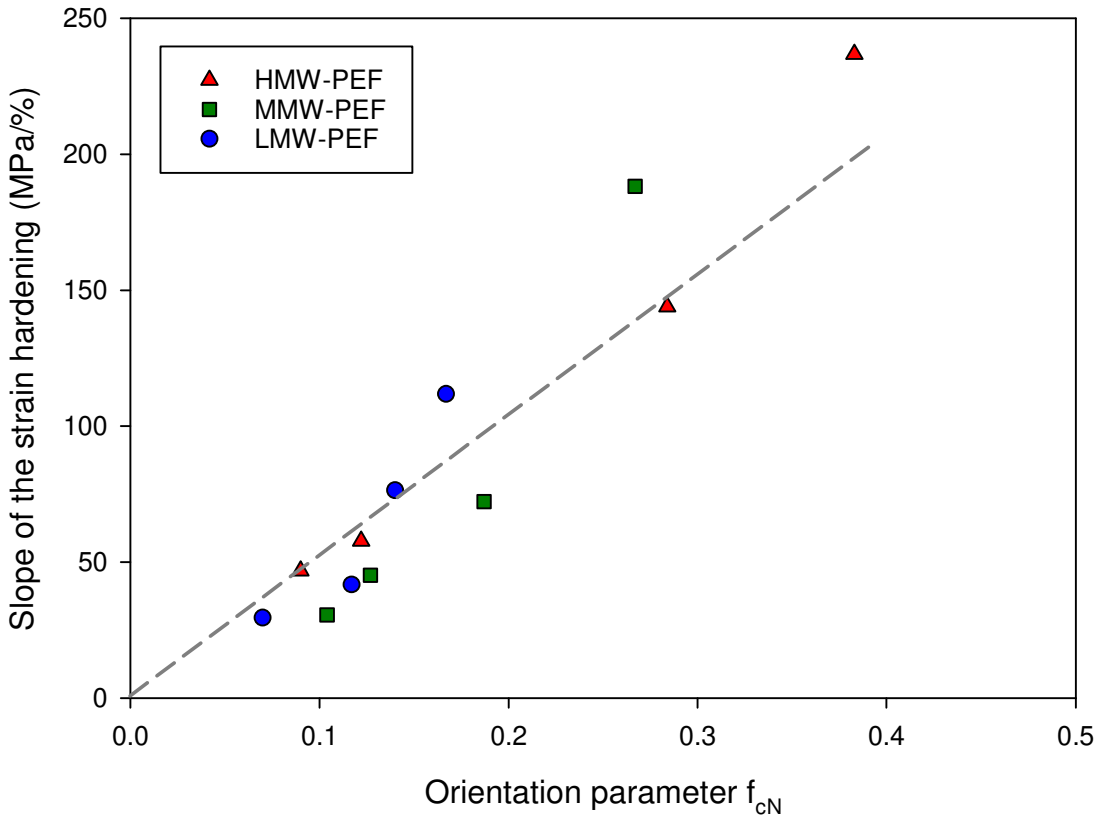

Figure 8 : Evolution of the strain-hardening slope as a function of the orientation parameter f_{cN} for LMW, MMW- and HMW-PEF (the slope of the strain hardening was determined in the $3x3 \leq \lambda x \lambda \leq 4.5x4.5$ region)

A reasonably good correlation is observed between f_{cN} and the slope of the strain-hardening except for high f_{cN} values (i.e., for high elongation ratios). This suggests that, in the case of PEF, strain-hardening mainly originates from the extension of the macromolecular network. Particularly, the increase of the amorphous phase orientation leads to an increase of the strain-hardening slope. This conclusion seems in opposition with the observations of PET where SIC is believed to be the predominant phenomenon at the origin of strain-hardening. However one have to keep in mind that in PEF the crystallinity achieved upon biaxial stretching is very low and that's why crystals play a modest role regarding the material stiffening. However, even if low crystal contents are induced, it can be seen that they play a role on macromolecular orientation as shown by the deviation from the two last point representing the higher orientation values. Particularly it can be assumed that, the strain-induced crystals plays the role of crosslinking/entanglement points which favor/force the amorphous macromolecular orientation.

Properties of BO films

The influence of molecular weight and biaxial stretching on some end-to-use properties of PEF have been determined. The oxygen permeability as a function of the biaxial elongation ratio are displayed in

(a) (b)

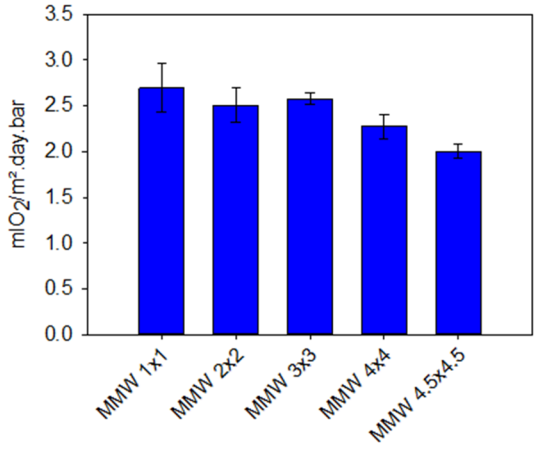

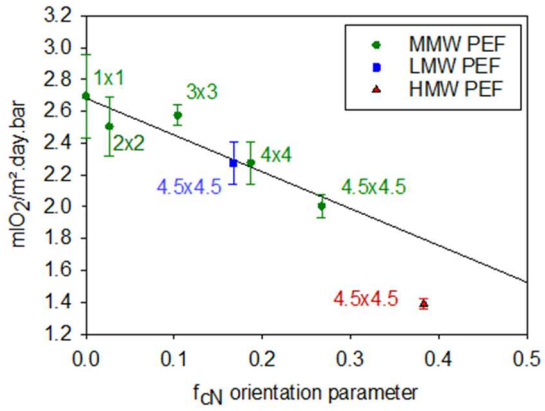

(c)

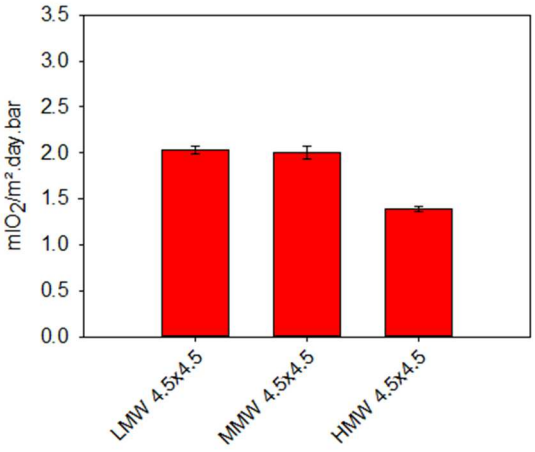

Figure 9.a and

(a)

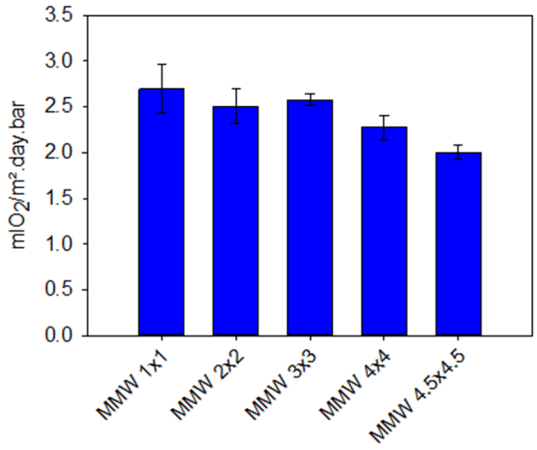

(b)

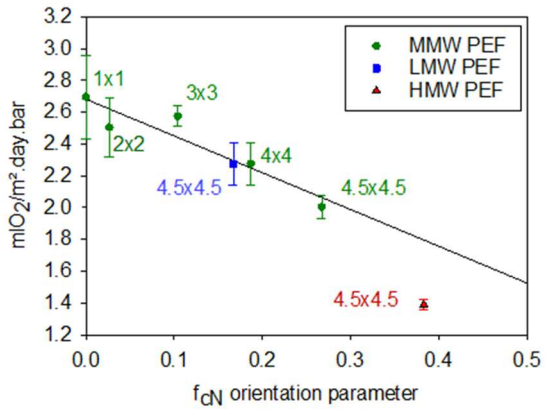

(c)

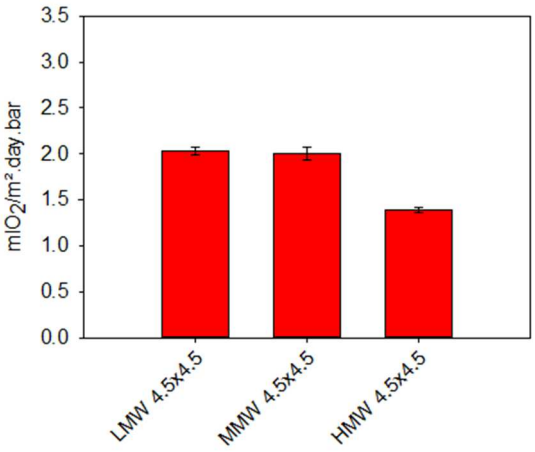

Figure 9.b while

(a)

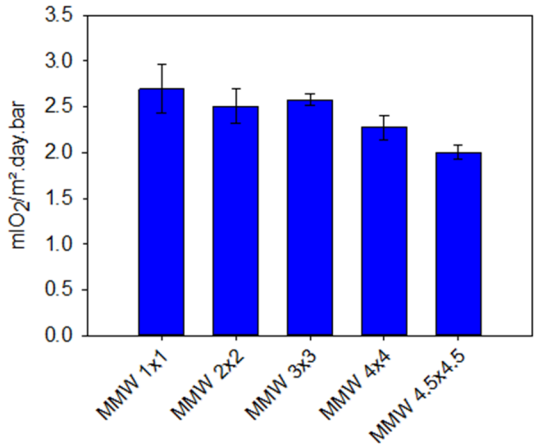
3.5
3.0
2.5
2.0
1.5
1.0
0.5
0.0
mlO2/m².day.bar
MMW 1x1
MMW 2x2
MMW 3x3
MMW 4x4
MMW 4.5x4.5

(b)

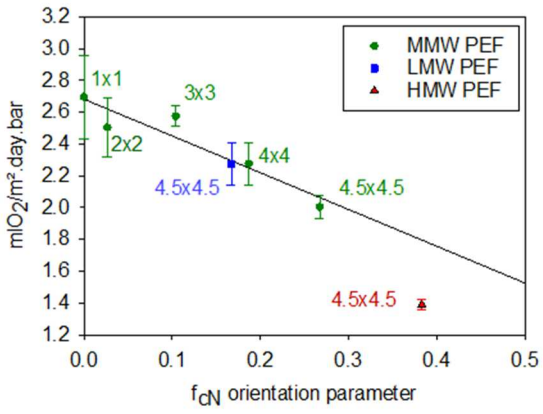
3.2
3.0
2.8
2.6
2.4
2.2
2.0
1.8
1.6
1.4
1.2
mlO2/m².day.bar
0.0
0.1
0.2
0.3
0.4
0.5
fcN orientation parameter
MMW PEF
LMW PEF
HMW PEF
1x1
2x2
3x3
4x4
4.5x4.5
4.5x4.5
4.5x4.5

(c)

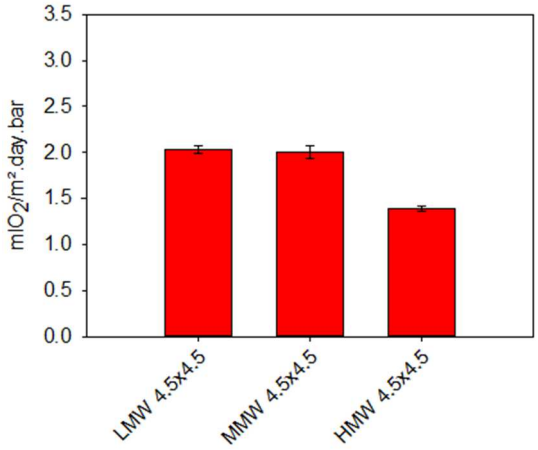

Figure 9.c depicts the effect of molecular weights on this property.

(a) (b)

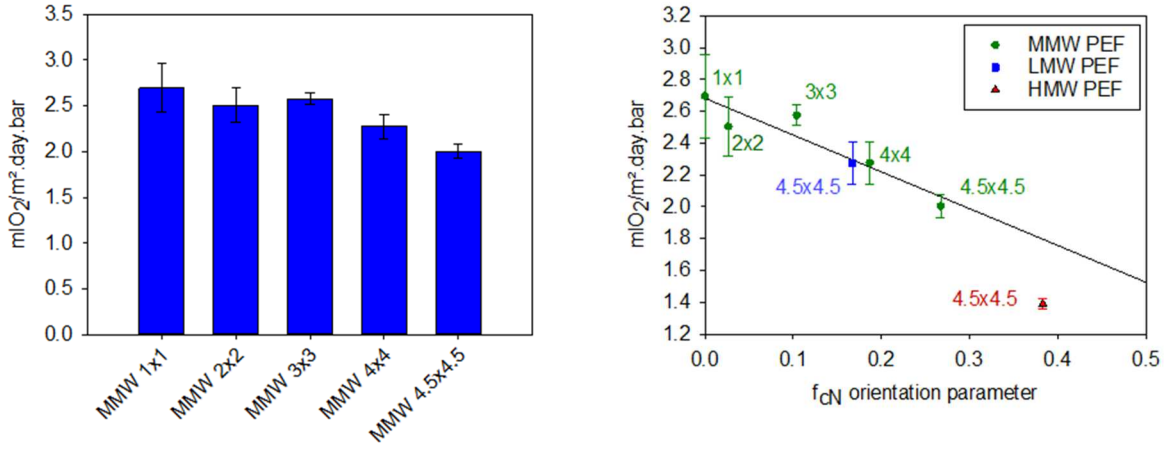

(c)

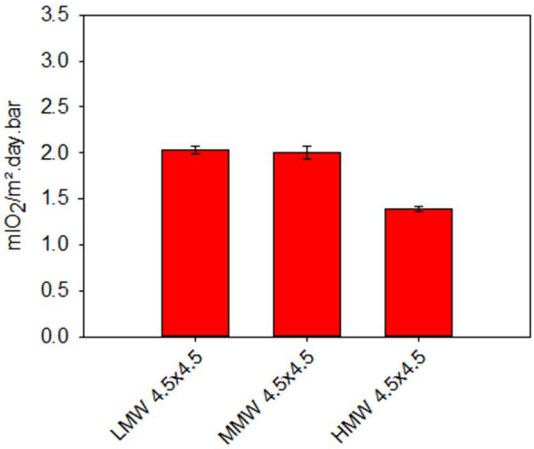

Figure 9 : (a) Oxygen Transmission Rate for cast and biaxially oriented PEF samples determined at equilibrium permeation at 23°C and 80%RH, (b) evolution of OTR as a function of the amorphous orientation parameter and (c) evolution of OTR as a function of molecular weight

Regarding the effect of the biaxial stretching ratio no significant effect is observed for draw ratios up to 3x3 while the OTR value decreases for higher elongation ratios. This stretching range where a decrease of the OTR value is measured corresponds to the range where strain-hardening is observed on the mechanical curves. To go further, the OTR values have been plotted as a function of the macromolecular orientation degree (

(a)

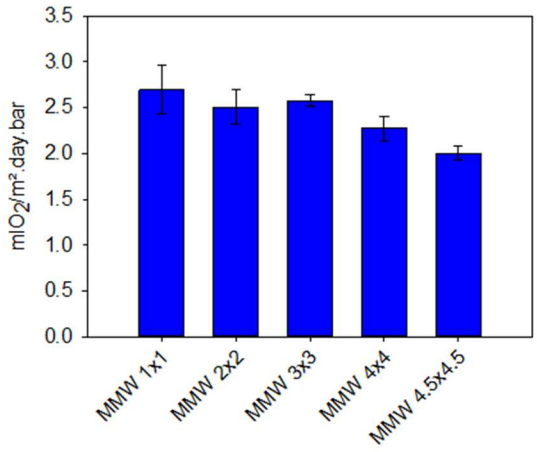
3.5
3.0
2.5
2.0
1.5
1.0
0.5
0.0
mlO2/m².day.bar
MMW 1x1
MMW 2x2
MMW 3x3
MMW 4x4
MMW 4.5x4.5

(b)

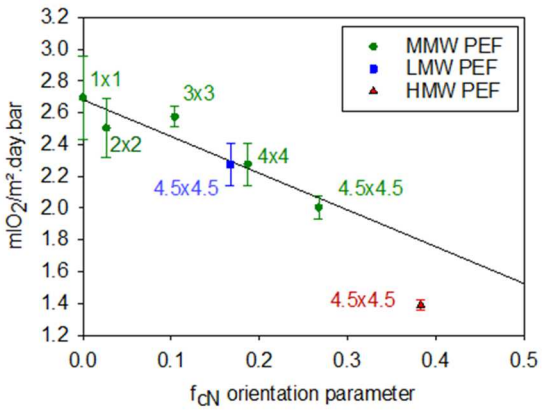
3.2
3.0
2.8
2.6
2.4
2.2
2.0
1.8
1.6
1.4
1.2
mlO2/m².day.bar
0.0
0.1
0.2
0.3
0.4
0.5
fcN orientation parameter
MMW PEF
LMW PEF
HMW PEF
1x1
2x2
3x3
4x4
4.5x4.5
4.5x4.5
4.5x4.5

(c)

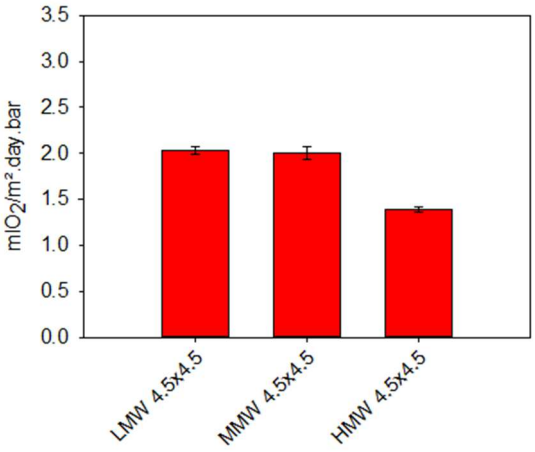
3.5
3.0
2.5
2.0
1.5
1.0
0.5
0.0
mlO2/m².day.bar
LMW 4.5x4.5
MMW 4.5x4.5
HMW 4.5x4.5

Figure 9.b). It appears that there's a good correlation between OTR value and macromolecular orientation. Considering that very low crystallinity is achieved in that case, it can be assumed that the improvement of barrier properties observed originates from macromolecular orientation.

Regarding the effect of molecular weight,

(a)

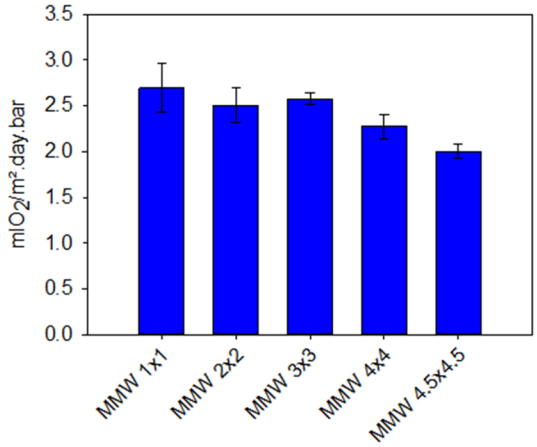

(b)

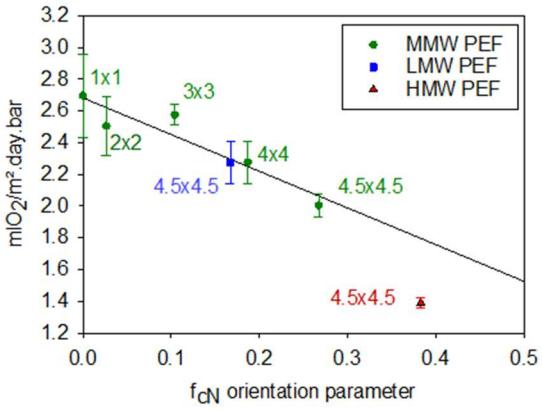

(c)

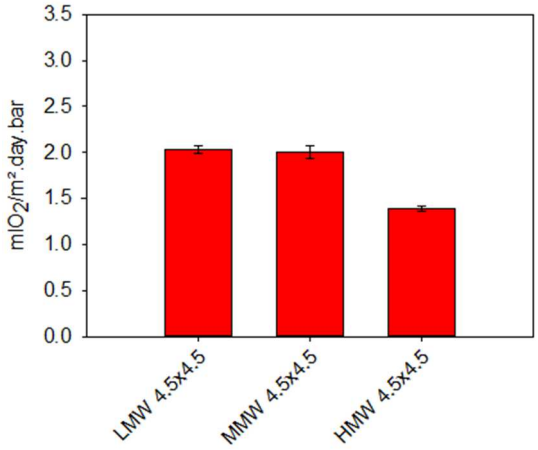

Figure 9.c shows that at λ x λ =4.5x4.5 there are no significant difference between LMW-PEF and MMW-PEF while HMW-PEF exhibits a lower value of OTR by 25%. Based on the WAXS analyses it has been shown that, at this draw ratio, both LMW-PEF and MMW-PEF exhibit no or very low crystallinity while a higher crystallinity degree was observed for HMW-PEF. This is confirmed by results from

(a) (b)

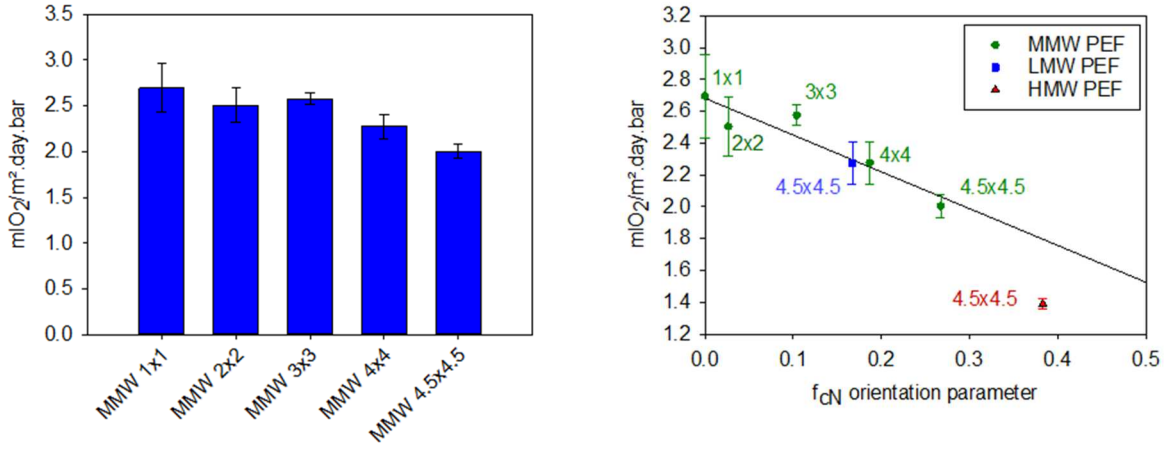

(c)

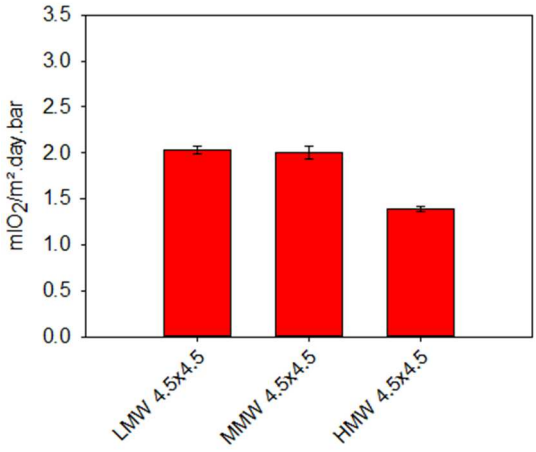

Figure 9.b. Indeed a linear correlation is observed between OTR and orientation parameters for samples exhibiting no or low crystallinity (i.e. LMW- and MMW-PEF). However, a strong deviation is observed for HMW-PEF which exhibits are moderate crystallinity degree. Consequently these data indicate that even if molecular orientation participates to the decrease of the oxygen permeability, crystallinity is a key parameter to improve the gas barrier properties of PEF.

Finally, the mechanical properties of cast-and BO films were tested through uniaxial tensile tests at room temperature. Both stress and strain at break of the as-cast and biaxially oriented films have been determined and are summarized in Figure 10.a and Figure 10.b respectively.

(a) (b)

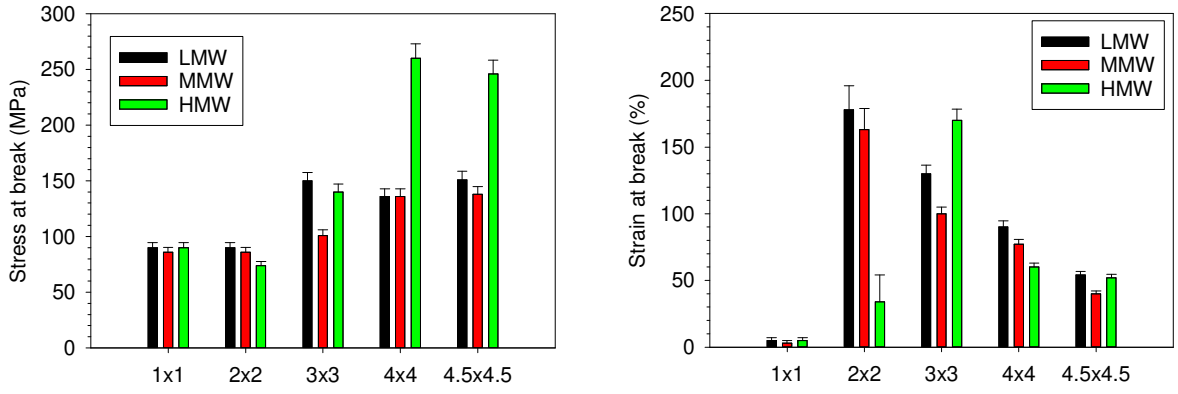

Figure 10 : Evolution of the (a) stress and (b) strain at break of as-cast and biaxially stretched PEF

Regarding stress at break, the trend is similar to what was observed for OTR measurements: there is no significant effect up to λxλ = 3x3, while an increase of the stress at break is observed for higher values. In addition this increase is fairly higher for HMW-PEF, probably due to the presence of a significant amount of crystal. On the other hand, an interesting feature is observed regarding the effect of biaxial stretching on the stretchability of PEF. Indeed, while the as-cast films are brittle, whatever the molecular weight, a ductile behavior is observed for elongation ratios above 2x2. Particularly, a strain at break as high as 170% can be achieved for LMW- and MMW- PEF when they are biaxially stretched at λxλ = 2x2. This brittle to ductile transition induced by biaxial stretching is of prime interest as it drastically improves the toughness of the PEF films. Finally it appears that, for λxλ ≥ 2x2, the strain at break decreases with the increase of the biaxial draw ratio. This is explained by the fact that the macromolecular orientation induced by biaxial stretching limits further elongation of the macromolecules during the uniaxial stretching test.

Origin of the brittle to ductile transition

Recently Xu et al. report a similar brittle to ductile transition induced by biaxial stretching in the case of Polylactide (PLA)[37]. In their study, authors show that this behavior transition is linked with a transition of the elementary plastic deformation mechanisms involved. Particularly they observed that the brittle behavior arises from the occurrence of crazing during stretching in the glassy state while shear banding is involved when the material is ductile. In addition they put in evidence that this brittle to ductile transition occurs when a critical molecular orientation parameter is reached, i.e. $f_{cM}=f_{cN}\approx0.07$ for PLA. In order to try to understand the origin of this brittle to ductile transition in the case of PEF, BO samples have been analyzed by means of SAXS (Figure 11).

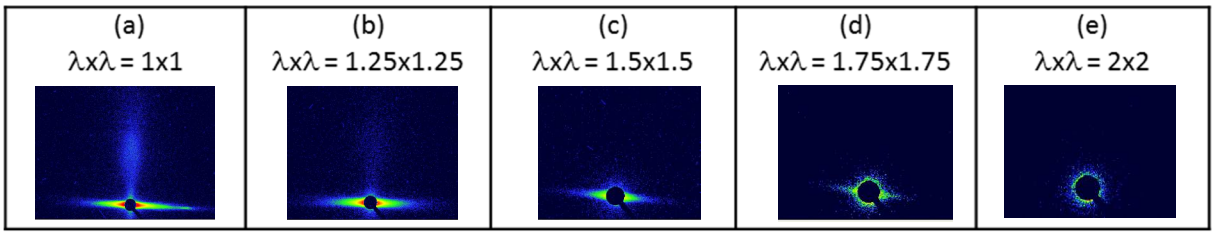

Figure 11 : (a-e) SAXS patterns of as-cast and BO MMW-PEF samples taken just before breaking during the uniaxial tensile test at room temperature (stretching axis is horizontal)

The SAXS pattern recorded for the cast-film (a) uniaxially drawn at room temperature clearly indicates that crazing is involved which explains the brittle behavior of the PEF cast-film. In opposition, for a MMW-PEF film biaxially drawn up to λxλ = 2x2 (e), there's no more evidence of the

presence of crazes. In addition, optical microscopy analyses revealed the presence of shear bands at the surface sample, explaining the ductile behavior observed (Figure 12). In order to assess the origin of this transition of plastic deformation mechanisms, MMW-PEF films were biaxially drawn at intermediates draw ratios between 1x1 and 2x2. The corresponding SAXS patterns (b-d) show a decrease of the scattered intensity with the increase of the draw ratio which is explained by a decrease of the crazes density. Consequently macromolecular orientation has an inhibiting or at least a restricting effect on the formation of crazes at the benefit of shear banding. Further investigations are under progress in order to determine how macromolecular orientation infers on the crazing mechanism.

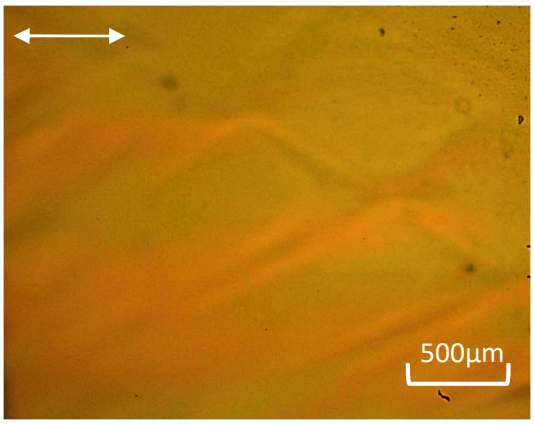

Figure 12. Optical observation of a MMW-PEF film pre-oriented at 2x2 after rupture upon uniaxial deformation.

Conclusion

The influence of the molecular weight on the mechanical behavior and associated structural evolution of PEF has been investigated. The influence of molecular weight on the mechanical behavior is limited as almost the same behavior is observed whatever the molecular weight. Particularly a strain-hardening stage is observed under appropriate biaxial stretching conditions, only the slope of strain hardening increases when increasing molecular weight. However, the molecular weight strongly influences the strain-induced structural evolution. Indeed while the low molecular weight PEF remains amorphous whatever the biaxial draw ratio, a strain-induced crystallization process is observed for higher molecular weights. This explains the higher slope of strain-hardening observed. To go further, the orientation degree of the macromolecules upon BO has been measured. Results indicate that strain-induced crystallization is driven by the orientation degree of the macromolecules. Particularly, a critical value of 0.18 has to be reach in order to initiate SIC. Even if SIC occurs, it was also shown that the mechanical behavior is mainly governed by the macromolecular orientation of the amorphous chains, due to the limited content of crystal induced. This faster macromolecular orientation kinetics for high molecular weight PEF is explained by the fact that long chains support more entanglements than small one, leading to a more constrained macromolecular network. Particularly, the disentanglement of the macromolecules is disfavored when the molecular weight increases.
The effect of biaxial stretching on the resulting properties has also been analyzed. On the one hand it was shown that strain-induced crystallization leads to better oxygen permeation properties. On the other hand it has been evidenced that, whatever the molecular weight, biaxial stretching at sufficient draw ratios (i.e. when a critical macromolecular orientation degree is attained) leads to ductile films. This brittle to ductile transition has been explained by a transition in terms of elementary plastic

deformation mechanisms from crazing to shear banding. Particularly, the increase of the orientation degree, limits or avoids crazing. Still regarding end-use properties, it has been shown that biaxial stretching has a positive effect on oxygen permeability. This improvement of barrier properties has been linked, on the one hand to the macromolecular orientation and, on the other hand, to the formation of crystals during stretching which strongly infers on this parameter.
Another result of this work is that while the increase of the molecular weight has a positive effect on SIC, the opposite is observed for thermally induced crystallization were the increase of the molecular leads to a decrease of the crystallization speed.
Finally, from a practical point of view, this work shows that a critical molecular weight has to be used, not for observing strain-hardening, but rather to allow strain-induced crystallization in order to improve the end-to use properties of the material.

Acknowledgement

This manuscript is a tribute to the 50 year anniversary of the French Polymer Group (Groupe Français des Polymères - GFP). The authors are indebted University of Lille and Région Haut-de-France for funding the PhD thesis. Financial support from Région Nord Pas-de-Calais and European FEDER for both biaxial stretching and SAXS laboratory equipment is also gratefully acknowledged.

Data availability

The raw/processed data required to reproduce these findings cannot be shared at this time due to legal or ethical reasons.

References

[1] Fei X., Wang, J., Zhu J., Wang ., Liu X. **(2020)**
Biobased poly(ethylene 2,5-furancoate): No longer an alternative, but an irreplaceable polyester in the polymer industry.
ACS Sustainable Chemistry and Engineering, 8(23), 8471-8485.
doi: 10.1021/acssuschemeng.0c01862

[2] Stoclet, G., Gobius Du Sart, G., Yeniad, B., De Vos, S., Lefebvre, J.M. **(2015)**
Isothermal crystallization and structural characterization of poly(ethylene-2,5-furanoate)
Polymer, 72, art. no. 17973, 165-176.
doi: 10.1016/j.polymer.2015.07.014

[3] Tsanaktsis, V., Papageorgiou, D.G., Exarhopoulos, S., Bikiaris, D.N., Papageorgiou, G.Z. **(2015)**
Crystallization and Polymorphism of Poly(ethylene furanoate)
Crystal Growth and Design, 15 (11), 5505-5512.
doi: 10.1021/acs.cgd.5b01136

[4] Papageorgiou, G. Z., Tsanaktsis, V., Bikiaris, D. N. **(2014)**
Synthesis of poly(ethylene furandicarboxylate) polyester using monomers derived from renewable resources: Thermal behavior comparison with PET and PEN.
Physical Chemistry Chemical Physics, 16(17), 7946-7958.
doi: 10.1039/c4cp00518j

[5] Codou A., Guigo N., van Berkel J., de Jong E., Sbirrazzuoli N. **(2014)**
Nonisothermal Crystallization Kinetics of biobased Poly(ethylene 2,5-furandicarboxylate) synthesized via direct esterification process.
Macromol. Chem. Phys., 215, 2065−2074.
doi: 10.1002/macp.201400316

[6] Papageorgiou G.Z., Tsanaktsis V., Bikiaris D.N. **(2014)**
Synthesis of poly(ethylene furandicarboxylate) polyester using monomers derived from renewable resources: thermal behavior comparison with PET and PEN.
Phys. Chem. Chem. Phys. 16:7946-7958.
doi: 10.1039/c4cp00518j

[7] van Berkel J., Guigo N., Kolstad J. J., Sipos L., Wang B., Dam M. A., Sbirrazzuoli N. **(2015)**
Isothermal crystallization kinetics of Poly (ethylene 2,5-furandicarboxylate).
Macromol. Mater. Eng, 300(4), 466-474.
doi: 10.1002/mame.201400376

[8] Knoop, R.J.I., Vogelzang, W., Van Haveren, J., Van Es, D.S. **(2013)**
High molecular weight poly(ethylene-2,5-furanoate); Critical aspects in synthesis and mechanical property determination
Journal of Polymer Science, Part A: Polymer Chemistry, 51 (19), pp. 4191-4199.
doi: 10.1002/pola.26833

[9] Burgess, S.K., Karvan, O., Johnson, J.R., Kriegel, R.M., Koros, W.J. **(2014)**
Oxygen sorption and transport in amorphous poly(ethylene furanoate)
Polymer, 55 (18), pp. 4748-4756.
doi: 10.1016/j.polymer.2014.07.041

[10] Burgess, S.K., Mikkilineni, D.S., Yu, D.B., Kim, D.J., Mubarak, C.R., Kriegel, R.M., Koros, W.J. **(2014)**

Water sorption in poly(ethylene furanoate) compared to poly(ethylene terephthalate). Part 1: Equilibrium sorption
Polymer, 55 (26), pp. 6861-6869.
doi: 10.1016/j.polymer.2014.10.047

[11] Burgess, S.K., Mikkilineni, D.S., Yu, D.B., Kim, D.J., Mubarak, C.R., Kriegel, R.M., Koros, W.J. **(2014)** Water sorption in poly(ethylene furanoate) compared to poly(ethylene terephthalate). Part 2: Kinetic sorption
Polymer, 55 (26), pp. 6870-6882.
doi: 10.1016/j.polymer.2014.10.065

[12] Menager, C., Guigo, N., Martino, L., Sbirrazzuoli, N., Visser, H., Boyer, S. A. E., Combeaud, C. **(2018)** Strain induced crystallization in biobased poly(ethylene 2,5-furandicarboxylate) (PEF); conditions for appearance and microstructure analysis.
Polymer, 158, 364-371.
doi: 10.1016/j.polymer.2018.10.054

[13] Stoclet, G., Lefebvre, J. M., Yeniad, B., Gobius du Sart, G.,de Vos, S. **(2018)**
On the strain-induced structural evolution of poly(ethylene-2,5-furanoate) upon uniaxial stretching: An in-situ SAXS-WAXS study.
Polymer, 134, 227-241.
doi: 10.1016/j.polymer.2017.11.071

[14] Mao, Y., Bucknall, D. G., Kriegel, R. M. **(2018)**
Synchrotron X-ray scattering study on amorphous poly(ethylene furanoate) under uniaxial deformation.
Polymer, 139, 60-67.
doi: 10.1016/j.polymer.2018.01.062

[15] Mao, Y., Bucknall, D. G., Kriegel, R. M. **(2018)**
Simultaneous WAXS/SAXS study on semi-crystalline poly(ethylene furanoate) under uniaxial stretching.
Polymer, 143, 228-236.
doi: 10.1016/j.polymer.2018.04.018

[16] Forestier, E., Combeaud, C., Guigo, N., Sbirrazzuoli, N., Billon, N. **(2020)**
Understanding of strain-induced crystallization developments scenarios for polyesters: Comparison of poly(ethylene furanoate), PEF, and poly(ethylene terephthalate), PET.
Polymer, 203, 122755
doi: 10.1016/j.polymer.2020.122755

[17] E. Forestier, C. Combeaud, N. Guigo, G. Monge, J.-M. Haudin, N. Sbirrazzuoli, N. Billon **(2020)**
Strain-induced crystallisation of poly(ethylene 2,5-furandicarboxylate). Mechanical and crystallographic analysis.
Polymer, 187, 122126.
doi: 10.1016/j.polymer.2019.122126

[18] E. Forestier, N. Guigo, C. Combeaud, N. Billon, N. Sbirrazzuoli **(2020)**
Conformational changes analysis of PEF (polyethylene 2,5-furandicarboxylate) and PET (polyethylene terephthalate) under uniaxial stretching.
Macromolecules, 53(19), 8693-8703.

[19] Van Berkel, J.G., Guigo, N., Kolstad, J.J., Sbirrazzuoli, N. **(2018)**
Biaxial Orientation of Poly(ethylene 2,5-furandicarboxylate): An Explorative Study
Macromolecular Materials and Engineering, 303 (3), art. no. 1700507,
doi: 10.1002/mame.201700507

[20] Tassin, J.-F., Vigny, M., Veyrat, D. **(1999)**
Biaxial stretching of pet films: A molecular description
Macromolecular Symposia, 147, pp. 209-220.
doi: 10.1002/masy.19991470121

[21] Adams, A.M., Buckley, C.P., Jones, D.P. **(2000)**
Biaxial hot drawing of poly(ethylene terephthalate): Measurements and modelling of strain-stiffening
Polymer, 41 (2), pp. 771-786.
doi: 10.1016/S0032-3861(98)00834-9

[22] Roland, C.M., Sonnenschein, M.F. **(1990)**
Thermal marking of amorphous poly(ethylene terephthalate)
American Chemical Society, Polymer Preprints, Division of Polymer Chemistry, 31 (2), pp. 382-383.

[23] Ray, I., Khastgir, D., Mukunda, P.G. **(1993)**
Effect of strain rate and temperature on stress-strain properties of EVA-LDPE blends and the mechanism of strain hardening
Die Angewandte Makromolekulare Chemie, 205 (1), pp. 59-74.
doi: 10.1002/apmc.1993.052050105

[24] Chandran, P., Jabarin, S. **(1993)**
Biaxial orientation of poly (ethylene terephthalate). part II: The strain–hardening parameter.
Advances in Polymer Technology, 12(2), 133-151.
doi:10.1002/adv.1993.060120203

[25] Ouchiar, S., Stoclet, G., Cabaret, C., Addad, A., Gloaguen, V. **(2016)**
Effect of biaxial stretching on thermomechanical properties of polylactide based nanocomposites
Polymer, 99, pp. 358-367.
doi: 10.1016/j.polymer.2016.07.020

[26] Delpouve, N., Stoclet, G., Saiter, A., Dargent, E., Marais, S. **(2012)**
Water barrier properties in biaxially drawn poly(lactic acid) films
Journal of Physical Chemistry B, 116 (15), pp. 4615-4625.
doi: 10.1021/jp211670g

[27] Chau, C.C., Li, J.C.M. **(2003)**
Cross deformation and stress relaxation of biaxially oriented polystyrene films
Journal of Polymer Science, Part B: Polymer Physics, 41 (7), pp. 687-700.
doi: 10.1002/polb.10416

[28] Zhang, X., Ajji, A. **(2003)**
Biaxial orientation behavior of polystyrene: Orientation and properties
Journal of Applied Polymer Science, 89 (2), pp. 487-496.
doi: 10.1002/app.12268

[29] Bonnebat, C., Roullet, G., de Vries, A.J**. (1981)**
Biaxially oriented poly(ethylene terephthalate) bottles: Effects of resin molecular weight on parison stretching behavior
Polymer Engineering & Science, 21 (4), pp. 189-195.
doi: 10.1002/pen.760210403

[30] G. Wypych **(2016)**
Handbook of *Polymers* - 2nd Edition
ChemTec Publishing, p405

[31] Stoclet, G., Gobius Du Sart, G., Yeniad, B., De Vos, S., Lefebvre, J. M. **(2015)**
Isothermal crystallization and structural characterization of poly(ethylene-2,5-furanoate).
Polymer, 72, 165-176.
doi:10.1016/j.polymer.2015.07.014

[32] R.M. Kriegel, R.D. Moffit, M.W. Schultheis, Y. Shi, X. You
WO2015031907, 2015

[33] Buckley, C.P., Lew, C.Y. **(2011)**
Biaxial hot-drawing of poly(ethylene terephthalate): An experimental study spanning the processing range
Polymer, 52 (8), pp. 1803-1810.
doi: 10.1016/j.polymer.2011.02.039

[34] Martins, C.I., Cakmak, M. **(2005)**
Large deformation mechano-optical and dynamical phase behavior in uniaxially stretched poly(ethylene naphthalate)
Macromolecules, 38 (10), pp. 4260-4273.
doi: 10.1021/ma047499s

[35] Araujo, C.F., Nolasco, M.M., Ribeiro-Claro, P.J.A., Rudić, S., Silvestre, A.J.D., Vaz, P.D., Sousa, A.F. **(2018)**
Inside PEF: Chain Conformation and Dynamics in Crystalline and Amorphous Domains
Macromolecules, 51 (9), pp. 3515-3526.
doi: 10.1021/acs.macromol.8b00192

[36] LeBourvellec, G., Monnerie, L., Jarry, J.P. **(1986)**
Amorphous orientation and induced crystallization in uniaxially stretched poly(ethylene terephthalate glycol)
Polymer, 27 (6), pp. 856-860.
doi: 10.1016/0032-3861(86)90294-6

[37] Xu S., Tahon J.F., De-Waele I., Stoclet G., Gaucher V. **(2020)**
Brittle-to-ductile transition of PLA: the influence of macromolecular orientation
eXPRESS Polymer Letters, 14 (11), 1037-1047
doi: 10.3144/expresspolymlett.2020.84

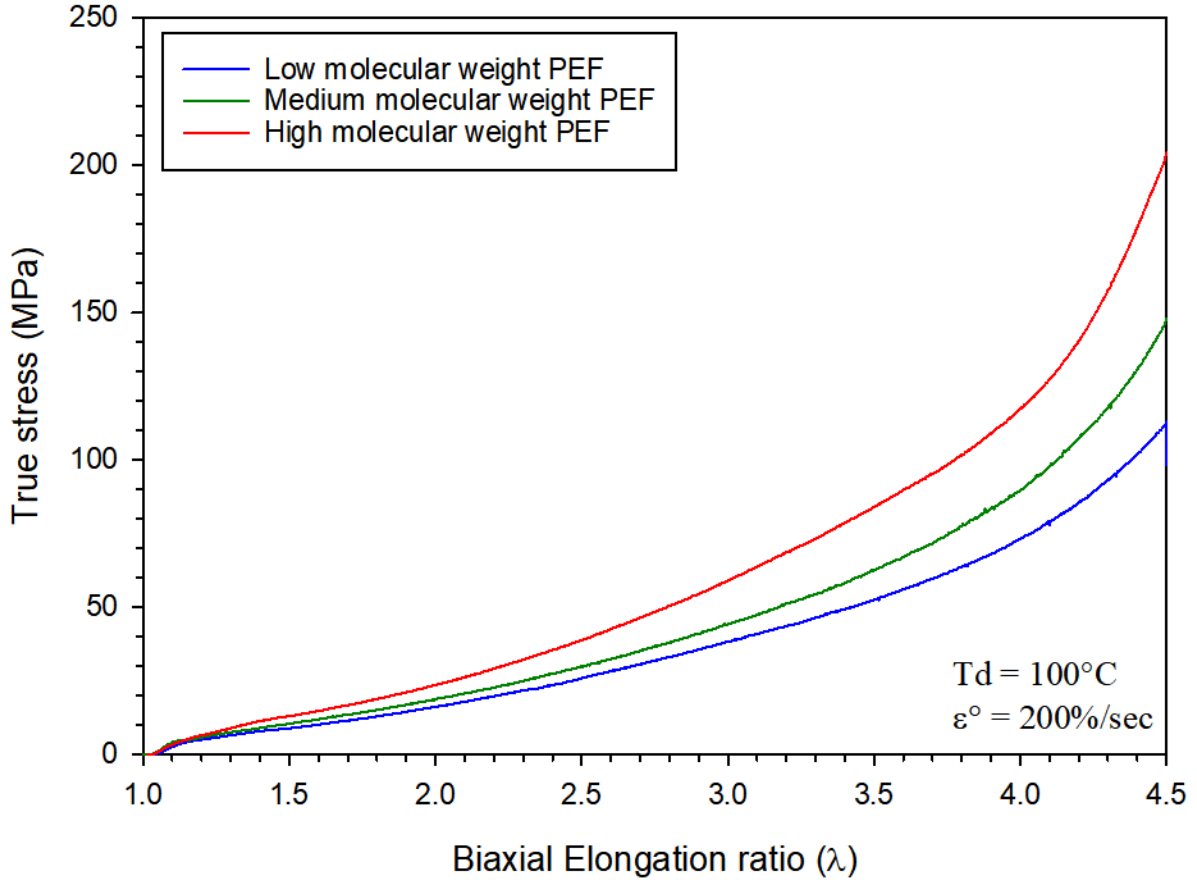
Low molecular weight PEF
Medium molecular weight PEF
High molecular weight PEF
Td = 100°C
ε° = 200%/sec
True stress (MPa)
Biaxial Elongation ratio (λ)
0
50
100
150
200
250
1.0
1.5
2.0
2.5
3.0
3.5
4.0
4.5

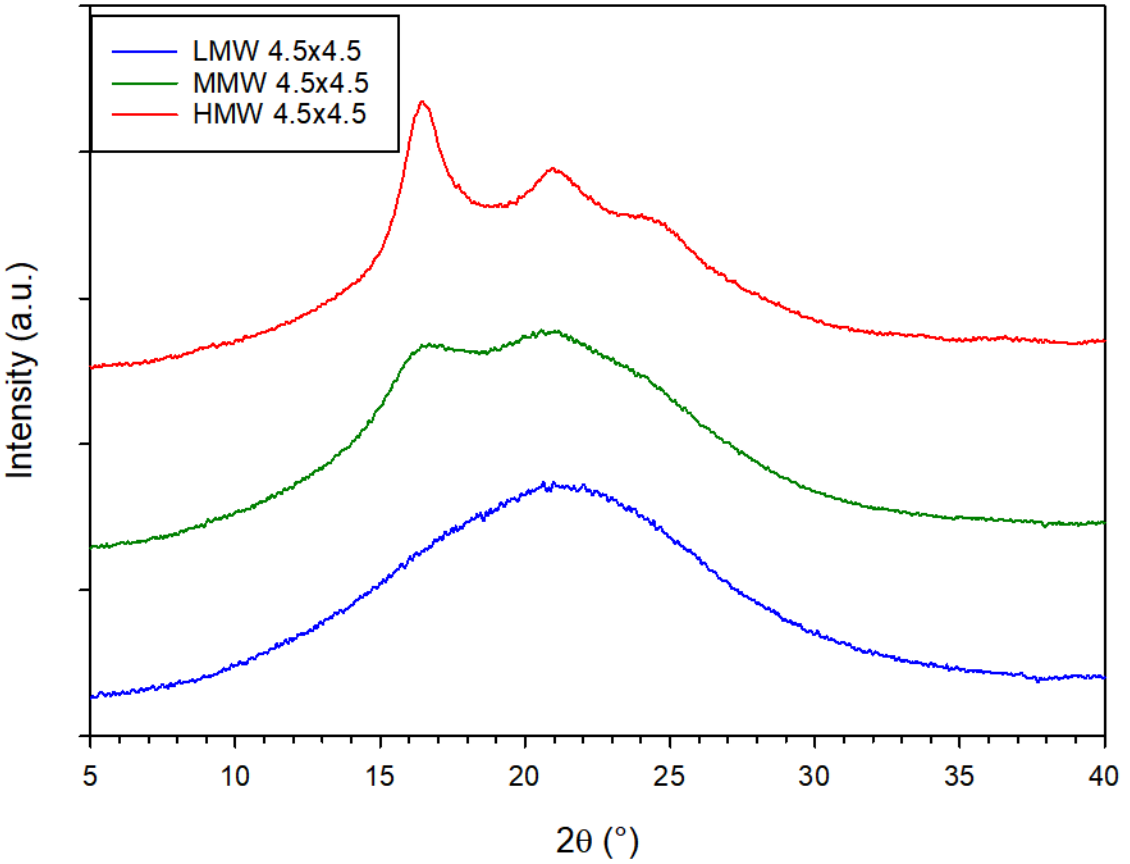
LMW 4.5x4.5
MMW 4.5x4.5
HMW 4.5x4.5
Intensity (a.u.)
2θ (°)
5
10
15
20
25
30
35
40